

EFFECT OF IRON ON ENERGY CONSUMPTION AND CURRENT EFFICIENCY OF ZINC ELECTROWINNING FROM SULFATE SOLUTIONS

Vanessa de Freitas Cunha Lins ¹

Renata Abelha ²

Maria das Mercês Reis de Castro ¹

Marina Maciel Dias de Souza ³

Leticia Lanza de Moraes ³

Carlos Roberto Araújo ⁴

Tulio Matencio ⁵

Abstract

Electrolytic zinc used in galvanizing processes is obtained using zinc electrowinning from sulfate solutions. The presence of impurities in the electrolyte is a major problem for the zinc electrowinning industry. The impurities on zinc electrolysis can reduce the current efficiency and increase the energy consumption. In this work, the effect of iron on the zinc electrodeposition using galvanostatic deposition and cyclic voltammetry is studied. Contents of 5, 10, and 15 mg.L⁻¹ of iron were added in the electrolyte of zinc sulfate and in an industrial acid electrolyte. Using the industrial electrolyte, iron addition is detrimental to the zinc electrowinning, increasing the energy consumption and decreasing the current efficiency.

Key words: Electrolysis; Energy consumption; Electrolytic zinc.

EFEITO DO FERRO NO CONSUMO DE ENERGIA E EFICIÊNCIA DE CORRENTE DA ELETRÓLISE DO ZINCO A PARTIR DE SOLUÇÕES SULFATADAS

Resumo

O zinco eletrolítico usado nos processos de galvanização é obtido através da eletrólise do zinco a partir de soluções sulfatadas. A presença de impurezas no eletrólito é o maior problema para a eletrólise do zinco industrial. As impurezas na eletrólise do zinco podem reduzir a eficiência de corrente e aumentar o consumo de energia. Neste trabalho é estudado o efeito do ferro na eletrodeposição do zinco, usando deposição galvanostática e voltametria cíclica. Foram adicionadas ao eletrólito de sulfato de zinco e a um eletrólito ácido industrial 5, 10 e 15 mg.L⁻¹ de ferro. No eletrólito ácido industrial a adição de ferro é prejudicial para a eletrólise do zinco, aumentando o consumo de energia e diminuindo a eficiência de corrente.

Palavras-chave: Eletrólise; Consumo de energia; Zinco eletrolítico.

I INTRODUCTION

One of the greatest changes in the last forty years concerning the application of steel as a structural element was the use of zinc coated steels for situations, which demand a high corrosion resistance. Galvanized steels can be applied in

all those industrial segments which normally use cold rolled steels such as the automotive industry, auto parts, metallic vehicle bodies, home appliances, electro-electronic equipment, steel furniture, civil construction and containers.⁽¹⁾

¹D.Sc., Associate Professor, Chemical Engineering Department, Federal University of Minas Gerais – UFMG. Antonio Carlos Avenue, 6627, Zip Code 31270-901, Belo Horizonte, MG, Brazil. E-mail: vlins@deq.ufmg.br

²M.Sc., Chemical Engineering Department, Federal University of Minas Gerais – UFMG.

Antonio Carlos Avenue, 6627, Zip Code 31270-901, Belo Horizonte, MG, Brazil. E-mail: renatabee@yahoo.com.br

³Undergraduate student, Chemical Engineering Department, Federal University of Minas Gerais – UFMG.

Antonio Carlos Avenue, 6627, Zip Code 31270-901, Belo Horizonte, MG, Brazil. E-mail: marinamacield@yahoo.com.br

⁴M.Sc., Professor, Pontifical Catholic University of Minas Gerais – PUC-MG.

Dom Jose Gaspar Avenue, 500, Zip Code 30535-901, Belo Horizonte, MG, Brazil. E-mail: carlosroberto_araujo@yahoo.com.br

⁵D.Sc., Associate Professor, Chemistry Department, Federal University of Minas Gerais – UFMG.

Antonio Carlos Avenue, 6627, Zip Code 31270-901, Belo Horizonte, MG, Brazil. E-mail: tmatencio@ufmg.br

One method of production of electrolytic zinc is electro-winning using sulfate solutions. The deposition of electrolytic zinc from alkaline zincate solution was investigated recently.^(2,3) Current is applied through insoluble electrodes and causes zinc deposition on cathode. Several parameters affect zinc electrolysis and its control.⁽⁴⁾ The presence of impurities in the electrolyte is a major problem for the zinc electrowinning industry.⁽⁵⁾ The synergistic interactions among impurities determine the quality of zinc deposit from the solution.⁽⁶⁾

Literature about the effect of impurities on zinc electro-winning is still scarce and restrict to specific impurities such as antimony,⁽⁷⁾ nickel,⁽⁸⁾ cadmium, iron and copper.⁽⁵⁾

A promising development in this area is the application of cyclic voltammetry and of electrochemical impedance spectroscopy to the investigation of the electrodeposition process.^(5,9)

The aim of this work is to study the effect of iron in the zinc electrowinning process using electrochemical techniques such as galvanostatic deposition and cyclic voltammetry. Two electrolytes were studied: a zinc sulfate electrolyte, pH 5.05, and an acid industrial electrolyte of zinc sulfate with addition of 180 g.L⁻¹ of H₂SO₄.

2 MATERIALS AND METHODS

Two electrolytes of zinc sulfate were used. A solution of 60 g.L⁻¹ of zinc was prepared dissolving 262.8 g of ZnSO₄.7H₂O in 1000 mL of deionized water. Solutions containing 60 g.L⁻¹ of zinc and 5, 10, and 15 mg.L⁻¹ of iron were prepared using ZnSO₄.7H₂O, FeSO₄.7H₂O, and deionized water.

Iron was added in a second electrolyte, used in an industrial plant of zinc electrowinning. Chemical characterization of this industrial acid electrolyte is shown in Table I. Chemical analysis was performed using the technique of atomic absorption spectrophotometry. Contents of 5 mg.L⁻¹, 10 mg.L⁻¹, and 15 mg.L⁻¹ were added in the industrial electrolyte.

Table I. Chemical composition of the industrial electrolyte

| Element | Content (g.L ⁻¹) |
|---------|------------------------------|
| Zn | 51.59 |
| Fe | 8.06.10 ⁻⁴ |
| Mn | 1.36 |
| Mg | 7.27 |
| Cd | 0.06 |

Electrochemical tests of galvanostatic deposition using a potentiostat/galvanostat AUTOLAB PGSTAT 30 were performed. Electrochemical cell was of three electrodes, an anode of Pb-Ag (1% wt), a cathode of aluminum and the reference electrode was Ag/AgCl. Zinc was deposited using galvanostatic deposition, applying a current density of 500 A.m⁻², which is used in the industrial plant of zinc electrolysis. A deposition time of 3 hours was used. Superficial area of cathode and anode was 1.0 cm². Before testing, cathodes were polished with 600-mesh sandpaper, washed in distilled water and dried. The zinc was removed from the cathode surface with a

stainless steel spatula. Zinc deposits were weighed in a precision balance for measurements of 0.0001 g. The aluminum cathode was also weighed before and after deposition (with the zinc deposits). Each experiment was performed five times.

Anderson-Darling normality analysis was performed to verify if the obtained data of deposited zinc mass have a normal distribution. F test of variance analysis (Minitab software, version 15) was used to verify the equality of media. Applying Faraday law, the theoretical mass of zinc was calculated using the equation:⁽¹⁰⁾

$$I = nF \frac{dn_i}{dt} = \frac{dQ}{dt} \quad (1)$$

where I is the electric current, in amperes, n is the moles of electrons, F is the Faraday constant, dni/dt represents the rate of reaction in moles per second, Q is the quantity of electricity or charge in coulombs (C), and t is the time. The theoretical zinc mass calculated was 184.71 mg. The current efficiency can be expressed by the ratio of deposited zinc mass and theoretical zinc mass.

Energy consumption (kWh/ton) was calculated using the expression:

$$\frac{Vm.8.4.10^5}{10.CE} \quad (2)$$

where Vm is the average potential (V), and CE the current efficiency (%).

Cyclic voltammetry tests were performed using a potentiostat/galvanostat AUTOLAB PGSTAT 30. Electrochemical cell was of three electrodes: an anode of aluminum, a counter electrode of platinum and the reference electrode was Ag/AgCl. Superficial area of cathode and anode was 1 cm². The scan rate was 10 mV.s⁻¹, and the potential range was from 0 to -1600 mV.

Characterization of the electrodeposited zinc was performed using scanning electron microscopy (SEM), and energy dispersive spectroscopy (EDS). Image analysis using Quantikov⁽¹¹⁾ software was carried out to evaluate porosity of the deposit.

3 RESULTS AND DISCUSSION

3.1 Current Efficiency and Energy Consumption

3.1.1 Electrolyte of acid solution

Table 2 shows current efficiency and energy consumption obtained in acid electrolytes without Fe and with additions of 5 mg.L⁻¹, 10 mg.L⁻¹, and 15 mg.L⁻¹ of Fe.

Table 2. Current efficiency and energy consumption of zinc electrowinning from acid solution

| Acid electrolyte | Cell voltage (mV _{Ag/AgCl}) | Electrodeposited zinc mass (mg) | Theoretical zinc mass (mg) | Current efficiency (%) | Energy consumption (kWh/T) |
|---|---------------------------------------|---------------------------------|----------------------------|------------------------|----------------------------|
| Without Fe | 1826 ± 4 | 654.8 ± 1.2 | 728 | 89.9 | 1705 |
| Addition of 5 mg.L ⁻¹ of Fe | 1835 ± 5 | 638.4 ± 0.9 | 728 | 87.7 | 1758 |
| Addition of 10 mg.L ⁻¹ of Fe | 1864 ± 5 | 641.5 ± 0.6 | 728 | 88.1 | 1777 |
| Addition of 15 mg.L ⁻¹ of Fe | 1896 ± 3 | 640.9 ± 0.6 | 728 | 88.0 | 1810 |

Iron addition is detrimental to the zinc electrowinning, increasing the energy consumption and decreasing the current efficiency. Among the solutions with iron addition, the addition of 10 mg.L⁻¹ produces the highest current efficiency.

3.1.2 Electrolyte of zinc sulfate

The addition of iron in the zinc sulfate electrolyte did not change the zinc mass deposited on cathode, and did not change the current efficiency, as shown in Table 3.

Table 3. Current efficiency and energy consumption of zinc electrowinning from zinc sulfate solution

| Zinc sulfate electrolyte | Cell voltage (mV _{Ag/AgCl}) | Electrodeposited zinc mass (mg) | Theoretical zinc mass (mg) | Current efficiency (%) | Energy consumption (kWh/T) |
|---------------------------|---------------------------------------|---------------------------------|----------------------------|------------------------|----------------------------|
| Without Fe | 2069 ± 3 | 182.4 ± 1.4 | 183 | 99.6 | 1744 |
| Addition of 5 mg/L of Fe | 2038 ± 4 | 182.1 ± 0.8 | 183 | 99.4 | 1722 |
| Addition of 10 mg/L of Fe | 2094 ± 5 | 182.5 ± 0.7 | 183 | 99.7 | 1765 |
| Addition of 15 mg/L of Fe | 2105 ± 5 | 182.1 ± 1.8 | 183 | 99.4 | 1778 |

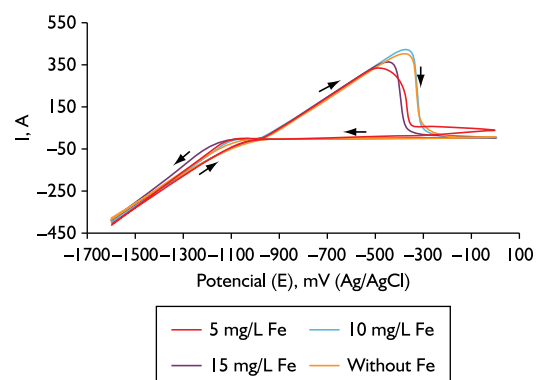
The addition of 5 mg.L⁻¹ of Fe decreases the energy consumption and the addition of 10, and 15 mg/L of Fe increases energy consumption (Table 3).

The current efficiency obtained using the electrolyte of zinc sulfate without H₂SO₄ addition, which is in the range of 99.5%, is higher than the current efficiency observed using the acid electrolyte, which was between 87.7% and 89.9%. For the electrolyte of zinc sulfate, the hydrogen reduction reaction did not compete significantly with zinc reduction. Over potential of zinc cathode increases with a decrease of pH.

3.2 Cyclic Voltammetry

3.2.1 Electrolyte of acid solution

Cyclic voltammetry experiments of zinc electrodeposition from 51.6 g.L⁻¹Zn, and 180 g.L⁻¹ of H₂SO₄ solution on aluminum substrate were carried out. The cathodic potential was varied in the range of 0 to -1600 mV (Ag/AgCl). The linear sweep curves that represent the onset of cathodic deposition and redissolution of deposited zinc are shown in Figure 1 for the solution without iron and with addition of 5 mg.L⁻¹, 10 mg.L⁻¹ and 15 mg.L⁻¹ of Fe.

**Figure 1.** Linear sweep curves that represent the onset of cathodic deposition and redissolution of deposited zinc are shown for the acid solution without iron addition and with 5 mg.L⁻¹, 10 mg.L⁻¹ and 15 mg.L⁻¹ of Fe.

The results are in good agreement with the results of galvanostatic deposition.

The cathodic curve can be attributed to the zinc deposition and hydrogen evolution reactions. Zinc deposition started at -1050 mV (Ag/AgCl). The anodic curves correspond to the dissolution of the deposited zinc. The current of anodic peak is higher for the electrolyte without iron and for the electrolyte with 10 mg.L⁻¹ of Fe, which also produced higher zinc mass electrodeposited in the galvanostatic deposition than the solutions with 5 and 15 mg.L⁻¹ of iron as shown in Table 2. The electrolytes without iron and the electrolyte with 10 mg.L⁻¹ of Fe showed anodic peaks at a higher potentials than the peaks for electrolytes with 5, and 15 mg.L⁻¹ of Fe. For a higher zinc mass dissolution, a higher current density and higher potentials were necessary. The two points of interception of curves with axis of abscise (zero current) determine the segment of the nucleation hysteresis loop. This segment is called BC.

No peak corresponding to Fe deposition is observed, probably because Fe does not adhere to the aluminum substrate and it is physically flushed away from the electrode surface by hydrogen evolution.

Figure 1 shows that for the acid electrolyte without iron, the BC portion decreases, indicating an acceleration of the cathodic process. In the presence of Fe, the nucleation/electrocrystallization overpotential (BC portion) increases, meaning that zinc deposition becomes more difficult in the presence of Fe. The addition of iron to the acid electrolyte produces an inhibition of the zinc deposition, which can be confirmed by the results of electrodeposited zinc mass as shown in Table 2. The inhibition of zinc reduction is due to the reduction of ferric ions, which is more significant as the iron content increases. The ferric ions were attracted to cathode and competed with zinc ions in the reduction process.

3.2.2 Electrolyte of zinc sulfate

The linear sweep curves that represent cathodic and anodic reactions for the zinc sulfate electrolyte are shown in Figure 2.

The electrolyte without iron addition shows a lowest current density of anodic peak. In this case, the zinc mass electrodeposited from an electrolyte without iron addition was the same mass deposited from an electrolyte with iron addition. A tendency of formation of a new anodic peak is observed at -50 mV (Ag/AgCl), and can be associated to the iron dissolution according to EDS results. The EDS analysis of the electrodeposited zinc shows the presence of iron in deposited zinc, for the electrolysis using the zinc sulfate with 10 and 15 mg.L^{-1} Fe.

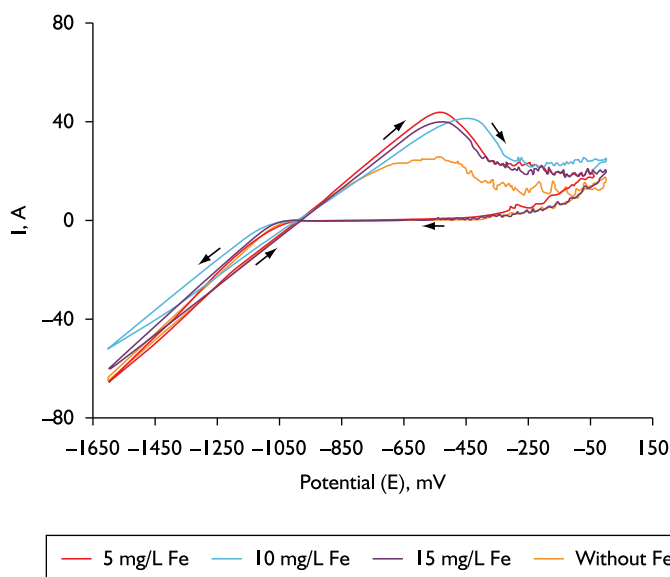


Figure 2. Linear sweep curves that represents the onset of cathodic deposition and redissolution of deposited zinc are shown for the zinc sulfate solution without iron addition and with 5 mg.L^{-1} , 10 mg.L^{-1} and 15 mg.L^{-1} Fe.

The BC regions in the voltammograms shown in Figure 2 are similar in length, indicating a same facility of the cathodic process. The values of electrodeposited zinc mass of the zinc sulfate electrolytes without iron, and with 5, 10, and 15 mg.L^{-1} Fe are similar, and are according to these results.

3.3 Morphology

3.3.1 Acid electrolyte

Morphology of electrodeposited zinc using acid electrolyte shows hexagonal crystals of zinc, deposited as multilayer, as shown in Figure 3, which presents a micrograph of surface of electrodeposited zinc using an acid electrolyte with 15 mg.L^{-1} Fe.

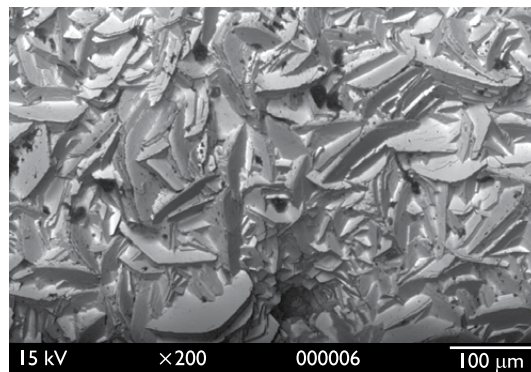


Figure 3. Micrograph of surface of electrodeposited zinc using an acid electrolyte with 15 mg.L^{-1} Fe.

EDS analysis of the electrodeposited zinc shows the presence of iron on deposited zinc using the acid electrolyte without iron addition (0.25 wt% Fe), and with 10 mg.L^{-1} Fe addition (0.11 wt% Fe). The acid industrial electrolyte contained iron as impurity before iron addition, according to Table 1. The electrodeposited zinc using the acid electrolyte without iron addition showed a higher mass than the deposited zinc obtained with acid electrolyte with addition of 5 and 15 mg.L^{-1} Fe.

The porosity of electrodeposited zinc does not change, or decreases with iron addition in acid electrolyte as shown in Table 4.

Table 4. Porosity of the electrodeposited zinc

| Electrolyte | Porosity (%) |
|-------------------------------------|--------------|
| 60 g/L Zn without Fe | 0.33 |
| 60 g/L Zn with 5 mg/L of Fe | 0.75 |
| 60 g/L Zn with 10 mg/L of Fe | 0.73 |
| 60 g/L Zn with 15 mg/L of Fe | 0.53 |
| Acid electrolyte | 0.65 |
| Acid electrolyte with 5 mg/L of Fe | 0.63 |
| Acid electrolyte with 10 mg/L of Fe | 0.38 |
| Acid electrolyte with 15 mg/L of Fe | 0.56 |

3.3.2 Zinc sulfate electrolyte

Morphology of the electrodeposited zinc consists of circular nodules of several diameters, as shown in Figure 4, which presents a surface of the electrodeposited zinc using a zinc sulfate electrolyte without iron addition.

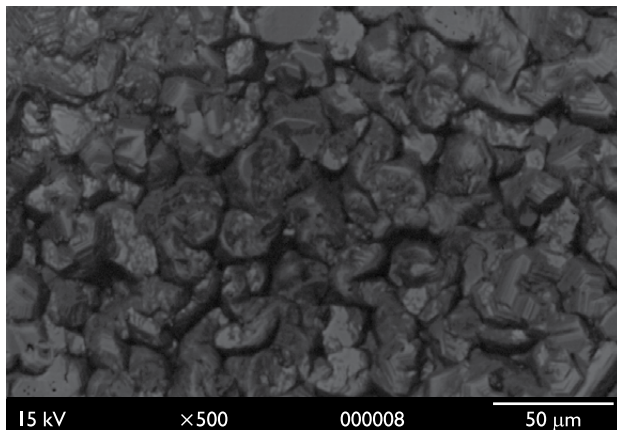


Figure 4. Morphology of the electrodeposited zinc consisting of circular nodules of several diameters obtained using the zinc sulfate electrolyte without iron addition.

Hexagonal crystals are not identified in deposits obtained using the zinc sulfate electrolyte without H_2SO_4 addition. Electrodeposited zinc by using an electrolyte of $Zn\ 60\ g.L^{-1}$ showed a content of sulfur of 2.5 wt% in a general surface analysis. Some sample surfaces showed dark regions with concentration of sulfur of 11.7 wt% (Figure 5).

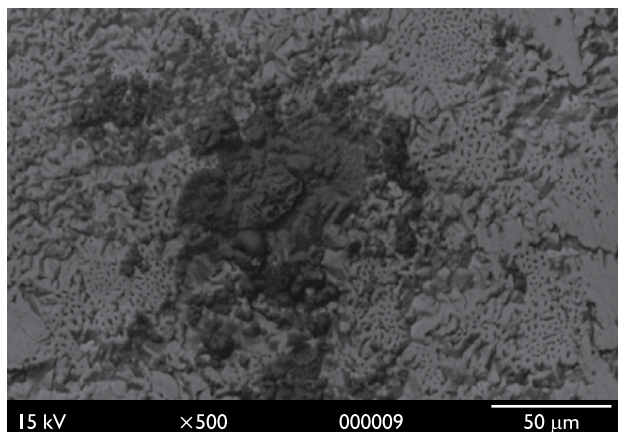


Figure 5. Surface of electrodeposited zinc obtained using a zinc sulfate electrolyte without iron addition, showing dark regions with sulfur enrichment.

The electrodeposited zinc with $5\ mg.L^{-1}$ Fe shows two different zinc electrodeposits. One zinc sheet was deposited, detached, and another zinc sheet was deposited. The edges of the first sheet shows cracks and sulfur enrichment (12 wt%). The first sheet showed a content of sulfur of 1.5 wt%, 0.9 wt% of Al, and a porosity of 0.75%. The second sheet shows a higher porosity than the first sheet (1.62%), a higher content of aluminum (2.1 wt%), and a lower content of sulfur (1 wt%).

The electrodeposited zinc with 10 and $15\ mg.L^{-1}$ Fe showed the presence of iron in deposit surface (0.94 and 0.10 wt%, respectively). Figure 6 shows a surface of electrodeposited zinc using the $60\ g.L^{-1}$ Zn electrolyte with $15\ mg.L^{-1}$ Fe. Some circular areas of a higher depth are observed on zinc surface (Figure 6).

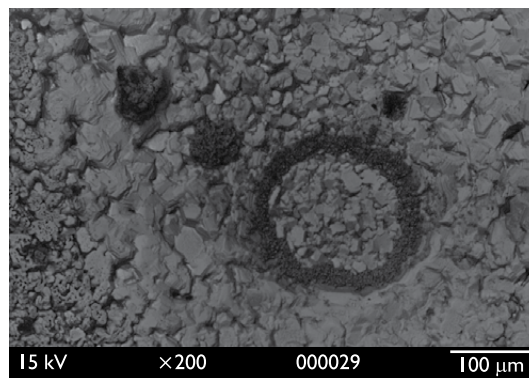


Figure 6. Surface of electrodeposited zinc using the $60\ g.L^{-1}$ Zn electrolyte with $15\ mg.L^{-1}$ Fe.

One result of the galvanostatic deposition of zinc using an electrolyte of $60\ g.L^{-1}$ Zn with $10\ mg.L^{-1}$ Fe is the deposition of two zinc sheets. The first sheet shows a porosity of 31.5% and a content of 5.0 wt% of sulfur. The second sheet shows a porosity of only 0.33%, and 3.1 wt% of sulfur.

The iron addition increases the porosity of electrodeposited zinc, using a $60\ g.L^{-1}$ Zn electrolyte, according to Table 4.

4 CONCLUSIONS

The current efficiency obtained using the electrolyte of zinc sulfate without H_2SO_4 addition, which is in the range of 99.5%, is higher than the current efficiency observed using the acid electrolyte, which is between 87.7% and 89.9%.

Using the acid electrolyte, iron addition is detrimental to the zinc electrowinning, increasing the energy consumption and decreasing the current efficiency.

The addition of iron in the zinc sulfate electrolyte does not change the current efficiency.

The addition of $5\ mg.L^{-1}$ of Fe in the zinc sulfate electrolyte decreases the energy consumption and the addition of 10, and $15\ mg.L^{-1}$ of Fe increases energy consumption.

The results of cyclic voltammetry indicate that the addition of iron to the acid electrolyte produces an inhibition of the zinc deposition, which can be confirmed by the results of electrodeposited zinc mass.

The addition of 5, 10 and 15mg.L⁻¹ of iron in zinc sulfate electrolyte produces a higher current density of anodic peaks in cyclic voltammograms, and a tendency of formation of a new anodic peak is observed at potential of - 50 mV (Ag/AgCl).

Morphology of electrodeposited zinc using the acid electrolyte shows hexagonal crystals of zinc, and the morphology of the zinc deposited using a 60 g.L⁻¹ Zn electrolyte consists of circular nodules.

The iron addition increases the porosity of electrodeposited zinc, using a 60 g.L⁻¹ Zn electrolyte.

Acknowledgements

Authors would like to thank to the governmental agencies National Council of Scientific and Technological Development, CNPq, Coordination of Improvement of Superior Level Staff, CAPES, and Foundation of Research Support of Minas Gerais State, FAPEMIG, and to the VOTORANTIM Industrial Group to support this research.

REFERENCES

- 1 LINS, V. F. C.; PARANHOS, R. M. V.; ALVARENGA, E. A. Behavior of the electrogalvanized and painted carbon steel and low Cu and Cr carbon steel during cyclic and field corrosion tests. *Journal of Materials Science*, v. 42, n. 13, p. 5094-104, 2007.
- 2 SHARIFI, B. *et al.* Effect of alkaline electrolysis conditions on current efficiency and morphology of zinc powder. *Hydrometallurgy*, v. 99, p. 72-6, 2009.
- 3 MOJTAHEDI, M. *et al.* Effect of electrolysis conditions of zinc powder production on zinc-silver oxide battery operation. *Energy Conversion and Management*, v. 52, n. 4, p. 1876-80, Apr. 2011.
- 4 GÜRMENT, S.; EMRE, M. A laboratory-scale investigation of alkaline zinc electrowinning. *Minerals Engineering*, v. 16, n. 6, p. 559-62, June 2003.
- 5 MURESAN L. *et al.* Influence of metallic impurities on zinc electrowinning from sulphate electrolyte. *Hydrometallurgy*, v. 43, n. 1-3, p. 345-54, Nov. 1996.
- 6 FOSNACHT, D. R.; O'KEEFE, T. Evaluation of zinc electrolytes containing certain impurities and additive by cyclic voltammetry. *Journal of Applied Electrochemistry*, v. 10, n. 4, p. 495-504, 1980.
- 7 IVANOV, I.; STEFANOV, Y. Electroextraction of zinc from sulphate electrolytes containing antimony ions and hydroxyethylated-butylene-2-diol-1,4: Part 3. The influence of manganese ions and a divided cell. *Hydrometallurgy*, v. 64, n. 3, p. 181-6, June 2002.
- 8 TRIPATHY, B. C.; DAS, S. C.; MISRA, V. N. Effect of antimony(III) on the electrocrystallisation of zinc from sulphate solutions containing SLS. *Hydrometallurgy*, v. 69, n. 1-3, p. 81-8, Apr. 2003.
- 9 ICHINO, R.; CACHET, C.; WIART, R. Influence of Ge⁴⁺ and Pb²⁺ ions on the kinetics of zinc electrodeposition in acidic sulphate electrolyte. *Journal of Applied Electrochemistry*, v. 25, n. 6, p. 556-64, 1995.
- 10 SABA, A. E.; ELSHERIEF, A. E. Continuous electrowinning of zinc. *Hydrometallurgy*, v. 54, n. 2-3, p. 91-106, Jan. 2000.
- 11 VASCONCELOS, D. C. L. *et al.* Influence of process parameters on the morphological evolution and fractal dimension of sol-gel colloidal silica particles. *Materials Science and Engineering A*, v. 334, n. 1-2, p. 53-8, Sep. 2002.

Recebido em: 23/09/2010

Aceito em: 18/02/2011